CircRNA UBAP2 Serves as a Sponge of miR-1294 to Increase Tumorigenesis in Hepatocellular Carcinoma through Regulating c-Myc Expression

Min-Cheng Yu
Zhongshan Hospital Fudan University
Guang-Yu Ding
Zhongshan Hospital Fudan University
Pei-Yao Fu
Zhongshan Hospital Fudan University
Peng Ma
Zhongshan Hospital Fudan University
Xiao-Dong Zhu
Zhongshan Hospital Fudan University
Jia-Bin Cai
Zhongshan Hospital Fudan University
Ying-Hao Shen
Zhongshan Hospital Fudan University
Jian Zhou
Zhongshan Hospital Fudan University
Jia Fan
Zhongshan Hospital Fudan University
Hui-Chuan Sun
Zhongshan Hospital Fudan University
Ming Kuang
Zhongshan Hospital Fudan University
Cheng Huang (huang.cheng@zs-hospital.sh.cn)
Zhongshan Hospital Fudan University

Research

Keywords: Circular RNA, Hepatocellular carcinoma, miRNA, c-Myc

Posted Date: August 2nd, 2020

DOI: https://doi.org/10.21203/rs.3.rs-49281/v1

Version of Record: A version of this preprint was published at Carcinogenesis on January 1st, 2021. See the published version at https://doi.org/10.1093/carcin/bgab068.

Abstract

Background: Circular RNAs (circRNAs) are a class of regulatory RNAs with complex roles in healthy and diseased tissues. However, the oncogenic role of circRNAs in hepatocellular carcinoma (HCC) remains poorly understood, including the mechanisms by which the circRNA UBAP2 contributes to tumorigenesis.

Methods: We analyzed the expression of circUBAP2 in 20 paired samples of HCC and healthy tissue as well as in seven HCC cell lines via quantitative real-time polymerase chain reaction (qRT-PCR). Functional experiments, such as CCK8 viability assays, colony formation assays, wound healing, transwell assays, and flow cytometry, were conducted to assess the effects of circUBAP2 *in vitro*. To further elucidate the mechanisms by which circUBAP2 acts, we conducted dual-luciferase assays, western blots, RNA pull-down assays, and rescue experiments.

Results: circUBAP2 was highly upregulated in most HCC tissues and was associated with poor prognosis. HCC patients with high circUBAP2 expression had greater vascular invasion and worse differentiation. Functionally, circUBAP2 overexpression enhanced HCC cell proliferation, migration, and invasion and inhibited apoptosis. Furthermore, we found that circUBAP2 upregulated c-Myc expression by sponging miR-1294, thus contributing to hepatocarcinogenesis. Inhibiting circUBAP2 expression in HCC attenuated the oncogenic effects of c-Myc.

Conclusions: These findings suggest that circUBAP2 promotes HCC growth and metastasis. circUBAP2 may have value as an independent prognostic biomarker or as a new target for the treatment of HCC.

Background

Hepatocellular carcinoma (HCC) is responsible for about 75-85% of primary liver cancers, which are the fourth most common cause of cancer-related death around the world[1, 2]. Despite great efforts of basic science and clinical research, HCC remains a highly deadly disease. Although HCC patients can be treated with surgery, tumor ablation, transarterial therapies, or systemic therapies (e.g. with tyrosine-kinase inhibitors or immune checkpoint inhibitors)[3], patients with advanced HCC lack effective options for therapeutic intervention, and prognoses are poor. A better understanding of the critical molecular events that occur in the pathogenesis of HCC may help uncover new biomarkers that can identify HCC patients who are at high risk of relapse. Further, a better understanding of the molecular process of disease may inform the rational design of effective therapeutics[4].

Circular RNAs (circRNAs), a type of noncoding, regulatory RNAs, are endogenous RNAs that have covalently linked ends[5]. These RNAs are mainly derived from the back-splicing of exons and are exceptionally stable due to their covalently closed ring structure[6-8]. Generally, circRNAs are expressed at low levels relative to their corresponding mRNAs and are primarily found in the cytoplasm of eukaryotic cells[9]. An increasing amount of evidence has suggested that circRNAs function as sponges that can protect specific mRNAs from miRNA-mediated degradation and as scaffolds that facilitate the colocalization of enzymes and their substrates, indirectly regulating protein activity[9, 10]. However, the

function of many circRNAs remains unknown[11]. Moreover, some circRNAs have been implicated in the progression of diseases such as diabetes mellitus, chronic inflammatory diseases, cardiovascular diseases, and neurological disorders. Emerging studies have focused on the importance of circRNAs in solid tumors, wherein circRNAs are generally categorized as oncogenes or tumor suppressors. Studies of the molecular mechanisms of circRNAs in HCC are still in their infancy. Understanding the role of circRNAs in the tumorigenesis and progression of HCC may facilitate the identification of therapeutic targets or potential biomarkers.

In this study, we found that circUBAP2 was markedly upregulated in HCC compared to paired healthy liver tissues. Further clinical analysis revealed that HCC patients with higher circUBAP2 expression tended to have worse prognoses. Additionally, functional studies suggested that circUBAP2 promoted tumorigenesis and progression in liver cancer by altering the circUBAP2/miR-1294/c-MYC signaling pathway. In summary, we identified circUBAP2 as an important regulator of the growth and metastasis of HCC, making it a promising therapeutic target for the management of HCC.

Materials And Methods

Patients and follow-up

HCC samples were collected from 125 patients diagnosed with HCC based on World Health Organization criteria at the Liver Cancer Institute, Zhongshan Hospital, Fudan University (Shanghai, China). All patients underwent curative resection at Zhongshan Hospital between February 2014 and January 2015. Follow-ups were performed after surgery and were completed by December 2019. Additionally, 20 pairs of HCC tissue and adjacent liver tissues were randomly selected to compare relative circUBAP2 levels. All collection of HCC tissues was performed according to a protocol approved by the institutional review board of Zhongshan Hospital, and each patient provided informed consent.

Cell lines and culture conditions

The human HCC cell lines used in these studies included MHCC97H, MHCC97L,HCCLM3, Huh-7, PLC/PRF/5, Hep-G2, and Hep-3B. The MHCC97H, MHCC97L, and HCCLM3 cell lines were developed at our institute. Huh-7 and PLC/PRF/5 cell lines were purchased from the Chinese Academy of Sciences. Hep-G2, and Hep-3B cell lines were purchased from the American Type Culture Collection and preserved at our institute. All cell lines were maintained in Dulbecco's modified Eagle's medium (DMEM) supplemented with 10% FBS in a humidified incubator at 37°C with 5% CO_2, as previously described.

CircRNA pull-down assay

CircRNA pull-down assays were conducted in accordance with the manufacturer's instructions. Biotin-labeled circUBAP2 and control probes were designed and synthesized by Sangon Biotech. Briefly, cell extracts were fixed with 1% formaldehyde, lysed, and sonicated. Then, each cell extract sample was centrifuged, and 50 μL of supernatant was retained. Next, the streptavidin-coupled Dynabeads were

added to the supernatant and incubated at 25°C for 1 hour. The complexes were then washed and incubated with lysis buffer and proteinase K. Finally, the RNA isolated from the pull-down bead sample was studied via qRT-PCR.

RNA immunoprecipitation (RIP)

RNA immunoprecipitation experiments were performed using an EZ-Magna RIP Kit in accordance with the manufacturer's instructions (Millipore, Billerica, MA, USA). Briefly, about 2×10^7 cells were collected and lysed in RIPA Lysis Buffer that contained proteinase and RNase inhibitors. Then, samples were incubated with the anti-AGO2 antibody (ab3238, Abcam) or IgG primary antibody (Cell Signaling Technology, USA). Twenty-four hours later, the complexes were washed five times with cold PBS. Finally, the immunoprecipitated RNAs were extracted and qRT-PCR was performed to detect RNA enrichment.

Luciferase assays

MHCC97H and HCCLM3 were cultured at 37°C with 5% CO_2 and were co-transfected with miR-1294 mimic, a luciferase reporter plasmid, and corresponding controls using Lipofectamine 2000. Forty-eight hours after transfection, luciferase activity was quantified using a Dual Luciferase Reporter Assay Kit (Yeasen) according to the manufacturer's protocol.

RNA extraction, qRT-PCR and western blot analysis

RNA isolation and qRT-PCR were performed as previously described[12]. Briefly, total RNA was extracted with Trizol reagent (Thermo Fisher, US). cDNA was synthesized using a PrimeScript RT reagent kit (Takara, Japan). Target genes were quantified using SYB Premix Ex Taq II (Takara, Japan). DNA amplification was performed using an ABI 7900 system. Western blots (WB) and immunohistochemistry staining were also performed as previously described[13].

Cell proliferation,colony formation, and invasion assays

To analyze cell proliferation and viability, we used Cell Counting Kit-8 (CCK-8) assays (Dojindo, Kumamoto, Japan) according to the manufacturer's instructions. Briefly, HCC cells were seeded into wells of 96-well plates (1×10^3 cells per well) and cultured at 37°C and 5% CO_2. Plates were monitored at the indicated times at an absorbance of 450 nm[14].

Colony formation assays were conducted as previously described[15]. Briefly, HCC cells (1×10^3 cells per well) were aliquoted into 6-well plates and cultured for 14 days. Colonies were then fixed with 100% methanol and stained with Giemsa staining solution (Sigma, USA). Visible colonies were counted using Image-Pro Plus 5.0 (Media Cybernetics, USA).

Invasion assays were conducted using transwell plates (Millipore, USA) coated with Matrigel (BD Biosciences, USA). DMEM containing 1% FBS was added to the upper chamber and DMEM containing 10% FBS was added to the lower chamber. HCC cells (2×10^5 per well) from each treatment group were

added to the upper chambers. After 48 hours of incubation, cells that invaded the lower chamber surface were fixed, stained with crystal violet (Sigma), and manually counted. All functional experiments were conducted in triplicate.

Xenograft mouse model

All *in vivo* experiments were performed in accordance with the Guide for the Care and Use of Laboratory Animals, as published by the US National Institutes of Health. All animal protocols were approved by the Animal Care Committee of Zhongshan Hospital. Briefly, 6-week-old nude mice, purchased from Charles River Laboratories (Beijing, China), were subcutaneously injected with 3×10^6 tumor cells. Tumor volumes and tumor weights were measured every 3 days. After 6 weeks, all mice were sacrificed for subsequent analyses.

Statistical analysis

All data were shown as the mean ± standard deviation of three independent experiments and were analyzed using SPSS 20.0 (SPSS, Chicago, IL, USA). We used t-tests, ANOVA, Mann-Whitney, chi-squared, and Fisher's exact tests to analyze differences between groups when appropriate. Time to reccurence (TTR) and overall survival (OS) were analyzed using Kaplan-Meier survival curves and log-rank tests, respectively. We also conducted univariate and multivariate analyses using Cox proportional hazard regression models. $P < 0.05$ was considered statistically significant.

Results

CircUBAP2 was upregulated in HCC tissues and indicated poor prognosis

To evaluate the relationship between circUBAP2 and outcomes among patients with HCC, we leveraged the StarBase database to perform bioinformatic analyses of the expression of circUBAP2 in HCC tissues. We found that circUBAP2 expression was significantly higher in HCC tissues relative to healthy liver tissues (Fig. 1B). In order to confirm the findings from the public database, we compared the relative expression of circUBAP2 in 20 paired formalin-fixed, paraffin-embedded tissue samples of liver cancer and adjacent healthy liver tissues via qRT-PCR (Fig. 1C). To investigate the diagnostic and prognostic value of circUBAP2 in HCC, we next measured the expression of circUBAP2 in 125 HCC tissues. Unexpectedly, we found that circUBAP2 was associated with markedly worse OS ($p < 0.001$) and TTR ($p < 0.001$) after surgical resection (Fig. 1D-E).

We investigated the association between the expression of circUBAP2 in HCC tissues and clinicopathological parameters through univariate and multivariate Cox proportional regression analyses. Multivariate subgroup analyses showed that high circUBAP2 expression was an independent factor for predicting both TTR [HR 2.83 (1.69-4.74), $p < 0.001$] and OS [HR 4.68 (2.45-8.89), $p < 0.001$, Tables 2-3]. Indeed, patients with higher circUBAP2 expression were more likely to have microvascular invasion (MVI) and worse differentiation (Tables 2-3).

We measured the relative expression of circUBAP2 in seven different characteristic HCC cell lines (Fig. 1F). In good agreement with our findings in patient samples, we found that circUBAP2 expression was higher in the high-grade malignancy cell lines HCCLM3 and MHCC97H relative to MHCC97L, a less malignant cell line, suggesting the cicrUBAP2 may facilitate the progression of HCC. Thus, we considered HCCLM3 and MHCC97H cells to be suitable for further experiments. These results collectively suggested that circUBAP2 is of significant importance in the pathogenesis of HCC.

CircUBAP2 promotes HCC cell proliferation and induces cell apoptosis

To investigate the biological effects of circUBAP2 in HCC cells, we generated two circUBAP2-specific shRNAs to target the back-splice sequence. As expected, these shRNAs led to downregulation of circUBAP2 expression in HCCLM3 and MHCC97H cell lines, as validated by qRT-PCR (Fig. 2A). We next performed a series of functional experiments. Here, we found that reduced circUBAP2 expression markedly suppressed cell proliferation (CCK8 assay, Fig. 2B-C). Consistently, flow cytometry assays showed that downregulation of circUBAP2 led to increased apoptosis in circUBAP2^{high} (Fig. 2D-E).

To further evaluate the function of circUBAP2 in vivo, we generated a xenograft tumor model using NOD/SCID/γc(null) (NOG) mice. We found that tumor volumes and weights were decreased in mice with down-regulated circUBAP2 relative to the control group (Fig. 2F). Further, the rate of tumor growth was significantly decreased (Fig. 2F).

CircUBAP2 promotes HCC cell migration and invasion

Pathological epithelial-mesenchymal transition (EMT) is a significant stage in cancer progression, in which cancer cells gain invasive potential[16]. Many important drivers of EMT, such as SNAIL1, bind to and suppress the activity of E-cadherin promoters and are correlated with increased chance of relapse and decreased survival in patients with HCC[17]. Notably, we found that, after knockdown of circUBAP2, HCCLM3 and MHCC97H had decreased migration in both transwell and wound healing assays (Fig. 3A-D). Moreover, in vitro transwell assays found decreased invasion of cells in the circUBAP2-KD group compared to the control group. Collectively, the above experiments confirmed that circUBAP2 promotes migration and invasion of HCC cells in vitro. To identify whether EMT was at the root of these malignant phenotypic changes, qRT-PCR and WB assays were performed to analyze changes in epithelial markers such as E-cadherin and mesenchymal markers such as N-cadherin and SNAIL1 (Fig. 3E-G). We found that circUBAP2-KD cell lines had decreased expression of N-cadherin and SNAIL1 compared with the mock-transfected cell lines. In accordance with the results from functional and molecular experiments, we found that circUBAP2 was associated with EMT and promoted migration and invasion of HCC cells.

circUBAP2 upregulated c-MYC expression by sponging miR-1294

Fluorescence in situ hybridization (FISH) and nuclear-plasma extraction assays suggested that circUBAP2 was primarily localized in the cytoplasm of the two HCC cell lines (Fig. 4A-B). A number of prior studies have reported that some circRNAs act as microRNA sponges. Accordingly, we conducted

dual-luciferase reporter assays to explore this possibility for circUBAP2. We constructed a luciferase report vector of wild-type (WT) and mutant (Mut) circUBAP2 and transfected that vector into both HCCLM3 and MHCC97H cell lines (Fig. 4C). After transfection, we found that overexpression of the miR-1294 mimic significantly reduced luciferase activity relative to the negative control (Fig. 4F). Furthermore, we performed RNA immunoprecipitation (RIP) studies with anti-Ago2 antibodies in the same two HCC cells and found that endogenous circUBAP2 was enriched (Fig. 4D). The results of a microRNA pull-down assay using biotin-labeled miR-1294 mimics showed significant enrichment of circUBAP2 compared with the control group (Fig. 4E). Meanwhile, a circRNA pull-down assay using a probe specific for circUBAP2 detected a clear increase in miR-1294 (Fig. 4D-E). Taken together, these results suggested that circUBAP2 functions as a sponge for miR-1294.

Next, we sought to determine the regulatory relationship and binding properties between miR-1294 and c-MYC through qRT-PCR (Fig. 4G), dual-luciferase reporter assays (Fig. 4H), and WB (Fig. 4I). We found that circUBAP2-KD cells had increased miR-1294 levels (Fig. 4G). Conversely, overexpression of miR-1294 reduced the expression of c-MYC protein (Fig. 4I). This result was confirmed by the reduced activity of a WT LUC-c-MYC reporter gene (Fig. 4H), however overexpression of miR-1294 had no effect on the activity of a LUC-c-MYC-mutant reporter gene (Fig. 4H). Collectively, these studies suggested that circUBAP2 may function as a sponge of miR-1294 to upregulate c-MYC expression.

miRNA inhibitor and overexpression of mRNA prevented the effects of circUBAP2 in liver cancer cells.

To further illustrate the regulatory interactions between circUBAP2 and miR-1294 that affect the c-MYC signaling pathway, we used a miR-1294 inhibitor to attenuate the induced expression in the initially circUBAP2 knockdown cells. qRT-PCR results confirmed that, as expected, addition of the miR-1294 inhibitor decreased the expression of miR-1294 in both MHCC97H and HCCLM3 cells (Fig. 5B). Of interest, we found that treatment with the miR-1294 inhibitor partially rescued the expression of c-MYC mRNA and protein relative to the control group (Fig. 5C-D). However, qRT-PCR analysis found that neither the addition of miR-1294 inhibitor nor the overexpression of c-MYC affected the expression of circUBAP2 (Fig. 5A).

Functional experiments revealed that the addition of miR-1294 inhibitor reversed the circUBAP2-knockdown-mediated increase in apoptosis and decrease in the proliferation, migration, and invasion in HCCLM3 and MHCC97H cells (Fig. 5E-H). Of note, the overexpression of c-MYC led to a reversal of the suppressive effects caused by circUBAP2 knockdown. circUBAP2-KD cells overexpressing c-MYC had significantly increased rates of proliferation and apoptosis, as determined by CCK8 and flow cytometry assays (Fig. 5E-F). Transwell migration and invasion assays showed attenuated motility and invasive potential in circUBAP2-KD cells, however these effects were partially reversed by overexpression of c-MYC (Fig. 5G-H). In summary, we determined that the addition of miR-1294 inhibitor and the overexpression of c-MYC reversed the oncogenic effects of circUBAP2 in HCC cells.

mRNA overexpression abolished the effects of miRNA on liver cancer cells.

In order to understand the exact interactions between miR-1294 and c-MYC, we transfected a miR-1294 mimic into MHCC97H and HCCLM3 cell lines. The effects of the miR-1294 mimic were confirmed by qRT-PCR in those two cell lines compared with a scrambled control miRNA mimic. Next, qRT-PCR was combined with WB assays to show that the overexpression of miR-1294 in MHCC97H and HCCLM3 cells led to decreased c-MYC expression (Fig. 6B-C). However, c-MYC overexpression did not alter miR-1294 expression in the same two cell lines (Fig. 5B). Therefore, we next tested whether c-MYC overexpression would attenuate the effects of miR-1294 in HCC cells. Indeed, overexpression of miR-1294 inhibited proliferation, migration, and invasion in MHCC97H and HCCLM3 cell lines (Fig. 6E-G). Conversely, when we also introduced c-MYC into the HCC cells, the tumor suppressive role of miR-1294 was significantly weakened. These findings matched with the finding of decreased cell viability, migration, and invasion (Fig. 6E-G). In summary, overexpression of c-MYC reversed the tumor suppressive role of miR-1294.

Discussion

Although the approach to management of HCC has changed dramatically over the last 5 years, outcomes remain poor. This may be because the main molecular drivers behind the transformation and progression of HCC have not yet been recognized[18]. CircRNAs are relatively new members of the noncoding cancer genome that have gene-regulatory potential and have been reported to drive malignant transformation and progression[19]. In recent years, there has been major progress in our understanding of the biogenesis and roles of circRNAs in HCC. An increasing number of studies indicate that circRNAs can play both oncogenic and tumor suppressive roles in HCC[20, 21]. Nevertheless, the vast majority of circRNAs in HCC have unknown functions, and the list of circRNAs involved in HCC continues to grow at a steady pace[19]. Previous studies have reported that circUBAP2 is important in the tumorigenesis and progression of esophageal squamous cell carcinoma[22], pancreatic adenocarcinoma[23], ovarian cancer[24], and osteosarcoma[25]. In this study, we found that circUBAP2 was aberrantly expressed in HCC tissues and was positively correlated with vascular invasion and worse differentiation. circUBAP2 functions as a sponge to inhibit the function of miR-1294, thus promoting HCC proliferation, invasion, and migration through the c-Myc signaling pathway. These findings suggested that circUBAP2 may hold promise as a biomarker or target for the management of HCC. However, further prospective cohort studies are required to validate the clinical value of circUBAP2.

Previous studies have reported that miR-1294 plays a critical role in osteosarcoma[26], gastric cancer[27], esophageal cancer[28], ovarian cancer[29], pancreatic ductal adenocarcinoma[30], clear cell renal cell carcinoma[31], and many other types of cancers. However, no prior studies have examined the role of miR-1294 in HCC. In this work, we found that knockdown of circUBAP2 enhanced the expression of miR-1294, and that upregulation of miR-1294 inhibited the growth and metastasis of HCC *in vitro* and *in vivo*. Moreover, we validated that the c-Myc oncogene was the target of miR-1294 through dual-luciferase reporter assays. Overexpression of c-Myc resulted in a reversal of the effects of miR-1294 in HCC cells. Future work will be needed to validate the clinical impacts of miR-1294 in HCC.

It has been firmly established that c-Myc acts as a pleiotropic transcription factor to control cell proliferation, apoptosis, metabolism, adhesion, DNA replication, differentiation, and angiogenesis[32-34]. The *c-Myc* oncogene is broadly overexpressed in many late-stage cancers and is often associated with tumorigenesis by causing inappropriate gene expression[35-37]. An increasing number of reports have recently focused on the role of c-Myc in HCC[38]. Mechanistically, our results suggested that knockdown of circUBAP2 led to a significant decrease in the expression of c-Myc in HCC and inhibited cellular DNA synthesis. Further, rescued expression of c-Myc in circUBAP2-KD cells promoted cellular proliferation and inhibited apoptosis. Previous reports have shown that c-Myc is a crucial factor in driving the transition from G0/G1 to the S phase in hepatocytes[39, 40]. We believe that our results suggest that circUBAP2 regulates HCC cell survival by affecting the c-Myc signaling pathway. Thus, inhibiting the expression of circUBAP2 may abolish the tumorigenesis of c-Myc, a previously undruggable target[41].

Conclusions

These experiments suggested that circUBAP2 has oncogenic potential in HCC. Specifically, circUBAP2 acts as a sponge of miR-1294 to upregulate c-Myc expression, which subsequently contributes to the activation of EMT signaling pathways and consequently promotes tumorigenesis and progression. Of note, circUBAP2 expression was a significant independent prognostic factor for TTR and OS. These findings may provide additional insights into the molecular events responsible for hepatocarcinogenesis. Further prospective studies will help determine the potential value of circUBAP2 as a prognostic indicator or therapeutic target for patients with HCC.

Abbreviations

HCC: Hepatocellular carcinoma; NOG: NOD/SCID/γc(null); circRNAs: circular RNAs; miRNAS: microRNAs; TTR: Time to recurrence; OS: Overall survival; EMT: Epithelial-mesenchymal transition; TMA: Tissue microarray analysis.

Declarations

Acknowledgement

Not applicable

Funding

This study was supported by the National Natural Science Foundation of China (No. 81871929).

Availability of data and materials

All data generated or analyzed during this study are included either in this article or in the Methods, Tables, Figures and Figure Legends files.

Authors' contributions

MCY, GYD, PYF, PM contributed to the development of methodology. XDZ, JBC, YHS and GYD contributed to the acquisition of data. MCY, GYD, PYF, YHS and GYD contributed to the interpretation of data and conducted the analysis. CH, MK, HCS, JF and JZ contributed to the design and conception of this study.

CH, MK, HCS, JF and JZ contributed to the review, and/or revision of the manuscript. CH and MK contributed to the administrative, technical, or material support. All authors read and approved the final manuscript.

Ethics approval and consent to participate

Ethical approval was obtained from the Zhongshan Hospital Research Ethics Committee, and written informed consent was obtained from each patient.

Consent for publication

Not applicable

Competing interests

The authors declare that they have no competing interests.

References

1. Singal AG, Lampertico P, Nahon P. Epidemiology and surveillance for hepatocellular carcinoma: New trends. Journal of hepatology. 2020;72:250-61.
2. Villanueva A. Hepatocellular Carcinoma. The New England journal of medicine. 2019;380:1450-62.
3. Forner A, Reig M, Bruix J. Hepatocellular carcinoma. Lancet (London, England). 2018;391:1301-14.
4. Rebouissou S, Nault JC. Advances in molecular classification and precision oncology in hepatocellular carcinoma. Journal of hepatology. 2020;72:215-29.
5. Ling H, Fabbri M, Calin GA. MicroRNAs and other non-coding RNAs as targets for anticancer drug development. Nature reviews Drug discovery. 2013;12:847-65.
6. Jeck WR, Sorrentino JA, Wang K, Slevin MK, Burd CE, Liu J, et al. Circular RNAs are abundant, conserved, and associated with ALU repeats. RNA (New York, NY). 2013;19:141-57.
7. Chen LL. The biogenesis and emerging roles of circular RNAs. Nature reviews Molecular cell biology. 2016;17:205-11.
8. Memczak S, Jens M, Elefsinioti A, Torti F, Krueger J, Rybak A, et al. Circular RNAs are a large class of animal RNAs with regulatory potency. Nature. 2013;495:333-8.
9. Li X, Yang L, Chen LL. The Biogenesis, Functions, and Challenges of Circular RNAs. Molecular cell. 2018;71:428-42.

10. Kristensen LS, Andersen MS, Stagsted LVW, Ebbesen KK, Hansen TB, Kjems J. The biogenesis, biology and characterization of circular RNAs. Nature reviews Genetics. 2019;20:675-91.
11. Han B, Chao J, Yao H. Circular RNA and its mechanisms in disease: From the bench to the clinic. Pharmacology & therapeutics. 2018;187:31-44.
12. Hu B, Sun D, Sun C, Sun YF, Sun HX, Zhu QF, et al. A polymeric nanoparticle formulation of curcumin in combination with sorafenib synergistically inhibits tumor growth and metastasis in an orthotopic model of human hepatocellular carcinoma. Biochemical and biophysical research communications. 2015;468:525-32.
13. Fu PY, Hu B, Ma XL, Tang WG, Yang ZF, Sun HX, et al. Far Upstream Element-Binding Protein 1 Facilitates Hepatocellular Carcinoma Invasion and Metastasis. Carcinogenesis. 2019.
14. Hu B, Ding GY, Fu PY, Zhu XD, Ji Y, Shi GM, et al. NOD-like receptor X1 functions as a tumor suppressor by inhibiting epithelial-mesenchymal transition and inducing aging in hepatocellular carcinoma cells. Journal of hematology & oncology. 2018;11:28.
15. Ma XL, Shen MN, Hu B, Wang BL, Yang WJ, Lv LH, et al. CD73 promotes hepatocellular carcinoma progression and metastasis via activating PI3K/AKT signaling by inducing Rap1-mediated membrane localization of P110beta and predicts poor prognosis. Journal of hematology & oncology. 2019;12:37.
16. Thiery JP, Acloque H, Huang RY, Nieto MA. Epithelial-mesenchymal transitions in development and disease. Cell. 2009;139:871-90.
17. Zeisberg M, Neilson EG. Biomarkers for epithelial-mesenchymal transitions. The Journal of clinical investigation. 2009;119:1429-37.
18. Bruix J, da Fonseca LG, Reig M. Insights into the success and failure of systemic therapy for hepatocellular carcinoma. Nature reviews Gastroenterology & hepatology. 2019;16:617-30.
19. Kristensen LS, Hansen TB, Veno MT, Kjems J. Circular RNAs in cancer: opportunities and challenges in the field. Oncogene. 2018;37:555-65.
20. Han D, Li J, Wang H, Su X, Hou J, Gu Y, et al. Circular RNA circMTO1 acts as the sponge of microRNA-9 to suppress hepatocellular carcinoma progression. Hepatology (Baltimore, Md). 2017;66:1151-64.
21. Hu ZQ, Zhou SL, Li J, Zhou ZJ, Wang PC, Xin HY, et al. Circular RNA Sequencing Identifies CircASAP1 as a Key Regulator in Hepatocellular Carcinoma Metastasis. Hepatology (Baltimore, Md). 2019.
22. Wu Y, Zhi L, Zhao Y, Yang L, Cai F. Knockdown of circular RNA UBAP2 inhibits the malignant behaviours of esophageal squamous cell carcinoma by microRNA-422a/Rab10 axis. Clinical and experimental pharmacology & physiology. 2020.
23. Zhao R, Ni J, Lu S, Jiang S, You L, Liu H, et al. CircUBAP2-mediated competing endogenous RNA network modulates tumorigenesis in pancreatic adenocarcinoma. Aging. 2019;11:8484-501.
24. Sheng M, Wei N, Yang HY, Yan M, Zhao QX, Jing LJ. CircRNA UBAP2 promotes the progression of ovarian cancer by sponging microRNA-144. European review for medical and pharmacological sciences. 2019;23:7283-94.

25. Zhang H, Wang G, Ding C, Liu P, Wang R, Ding W, et al. Increased circular RNA UBAP2 acts as a sponge of miR-143 to promote osteosarcoma progression. Oncotarget. 2017;8:61687-97.
26. Zhang ZF, Li GR, Cao CN, Xu Q, Wang GD, Jiang XF. MicroRNA-1294 targets HOXA9 and has a tumor suppressive role in osteosarcoma. European review for medical and pharmacological sciences. 2018;22:8582-8.
27. Shi YX, Ye BL, Hu BR, Ruan XJ. Expression of miR-1294 is downregulated and predicts a poor prognosis in gastric cancer. European review for medical and pharmacological sciences. 2018;22:5525-30.
28. Liu K, Li L, Rusidanmu A, Wang Y, Lv X. Down-Regulation of MiR-1294 is Related to Dismal Prognosis of Patients with Esophageal Squamous Cell Carcinoma through Elevating C-MYC Expression. Cellular physiology and biochemistry : international journal of experimental cellular physiology, biochemistry, and pharmacology. 2015;36:100-10.
29. Zhang Y, Huang S, Guo Y, Li L. MiR-1294 confers cisplatin resistance in ovarian Cancer cells by targeting IGF1R. Biomedicine & pharmacotherapy = Biomedecine & pharmacotherapie. 2018;106:1357-63.
30. Xu Y, Yao Y, Gao P, Cui Y. Upregulated circular RNA circ_0030235 predicts unfavorable prognosis in pancreatic ductal adenocarcinoma and facilitates cell progression by sponging miR-1253 and miR-1294. Biochemical and biophysical research communications. 2019;509:138-42.
31. Pan W, Pang LJ, Cai HL, Wu Y, Zhang W, Fang JC. MiR-1294 acts as a tumor suppressor in clear cell renal cell carcinoma through targeting HOXA6. European review for medical and pharmacological sciences. 2019;23:3719-25.
32. Whitfield JR, Soucek L. Tumor microenvironment: becoming sick of Myc. Cellular and molecular life sciences : CMLS. 2012;69:931-4.
33. Meyer N, Penn LZ. Reflecting on 25 years with MYC. Nature reviews Cancer. 2008;8:976-90.
34. Miller DM, Thomas SD, Islam A, Muench D, Sedoris K. c-Myc and cancer metabolism. Clinical cancer research : an official journal of the American Association for Cancer Research. 2012;18:5546-53.
35. Wu CH, van Riggelen J, Yetil A, Fan AC, Bachireddy P, Felsher DW. Cellular senescence is an important mechanism of tumor regression upon c-Myc inactivation. Proceedings of the National Academy of Sciences of the United States of America. 2007;104:13028-33.
36. Hsieh AL, Dang CV. MYC, Metabolic Synthetic Lethality, and Cancer. Recent results in cancer research Fortschritte der Krebsforschung Progres dans les recherches sur le cancer. 2016;207:73-91.
37. Dang CV, Reddy EP, Shokat KM, Soucek L. Drugging the 'undruggable' cancer targets. Nature reviews Cancer. 2017;17:502-8.
38. Zheng K, Cubero FJ, Nevzorova YA. c-MYC-Making Liver Sick: Role of c-MYC in Hepatic Cell Function, Homeostasis and Disease. Genes. 2017;8.
39. Thompson NL, Mead JE, Braun L, Goyette M, Shank PR, Fausto N. Sequential protooncogene expression during rat liver regeneration. Cancer research. 1986;46:3111-7.

40. Fausto N, Mead JE, Braun L, Thompson NL, Panzica M, Goyette M, et al. Proto-oncogene expression and growth factors during liver regeneration. Symposium on Fundamental Cancer Research. 1986;39:69-86.
41. Whitfield JR, Beaulieu ME, Soucek L. Strategies to Inhibit Myc and Their Clinical Applicability. Frontiers in cell and developmental biology. 2017;5:10.

Tables

Table 1.

Correlation between clinicopathological parameters of patients enrolled

Variables		Whole cohort (n=125)		
		Low circUBAP2 (n=62)	High circUBAP2 (n=63)	P
Sex	Female	12	19	0.162
	Male	50	44	
Age	≤50 year	24	31	0.237
	>50 year	38	32	
ALT	≤40 U/L	45	45	0.886
	>40 U/L	17	18	
AFP	≤400 ng/ml	47	49	0.794
	>400 ng/ml	15	14	
Cirrhosis	No	11	16	0.298
	Yes	51	47	
Tumor size	≤5 cm	40	39	0.762
	>5 cm	22	25	
Number	Single	55	54	0.616
	Multiple	7	9	
MVI	Absent	40	27	0.015
	Present	22	36	
Encapsulation	Complete	31	43	0.038
	Incomplete	31	20	
Differentiation	I-II	46	34	0.019
	III-IV	16	29	
BCLC	0+A	53	51	0.498
	B+C	9	12	

Abbreviations: HR, hazard ratio; HBsAg, hepatitis B surface antigen; ALT, alanine aminotransferase; AFP, α-fetoprotein; STIP1, Stress Induced Phosphoprotein 1; MVI, microvascular invasion

Table 2.

Univariate cox proportional regression analysis of factors associated with recurrence and overall survival

	Recurrence		Overall survival	
Variables	HR (95% CI)	*P*	HR (95% CI)	*P*
Age (>50y versus ≤50y)	0.82 (0.52-1.29)	0.385	0.70 (0.41-1.19)	0.187
Sex (male versus female)	0.77 (0.46-1.29)	0.317	0.55 (0.31-0.98)	0.042
Liver cirrhosis (yes versus no)	1.17 (0.66-2.07)	0.585	0.84 (0.45-1.57)	0.585
ALT (>40U/L versus ≤40U/L)	1.80 (1.11-2.90)	0.016	1.70 (0.97-2.98)	0.066
AFP (>400ng/ml versus ≤400ng/ml)	2.20 (1.35-3.60)	0.002	2.04 (1.05-3.84)	0.034
No. of tumors (multi versus single)	1.75 (0.96-3.14)	0.070	2.14 (1.07-4.69)	0.041
Tumor size (>5cm versus ≤5cm)	2.42 (1.52-3.83)	<0.001	1.56 (0.91-2.68)	0.106
Macro vascular invasion (yes versus no)	2.41 (1.15-5.03)	0.020	2.62 (1.18-5.81)	0.018
Micro vascular invasion (yes versus no)	1.87 (1.18-2.96)	0.008	1.96 (1.03-3.73)	0.040
Edmondson stage (III-IV versus I-II)	1.73 (1.09-2.74)	0.019	1.48 (0.86-2.55)	0.158
BCLC stage (B+C versus 0+A)	1.88 (1.10-3.22)	0.021	1.64 (0.88-3.07)	0.122
circUBAP2 (high versus low)	2.40 (1.50-3.84)	<0.001	4.31 (2.30-8.09)	<0.001

Abbreviations: ALT, alanine aminotransferase; AST, aspartate transaminase; AFP, α-fetoprotein; BCLC, Barcelona Clinic Liver Cancer; HR, hazard ratio; N.A, not applicable.

Table 3.
Multivariate cox proportional regression analysis of factors associated with recurrence and overall survival

	Recurrence		Overall survival	
Variables	HR (95% CI)	*P*	HR (95% CI)	*P*
AFP (>400ng/ml versus ≤400ng/ml)	2.47 (1.42-4.29)	0.001	2.18 (1.18-4.03)	0.013
ALT (>40U/L versus ≤40U/L)	1.46 (0.88-2.44)	0.145	N.A.	
Tumor size (>5cm versus ≤5cm)	2.05 (1.23-3.42)	0.006	N.A.	
No. of tumors (multi versus single)	N.A.		1.44 (0.69-3.01)	0.338
Macro vascular invasion (yes versus no)	1.15 (0.50-2.62)	0.744	1.95 (0.83-4.57)	0.124
Micro vascular invasion (yes versus no)	0.98 (0.58-1.67)	0.943	1.09 (0.59-2.00)	0.784
Edmondson stage (III-IV versus I-II)	1.28 (0.78-2.10)	0.339	N.A.	
circUBAP2 (high versus low)	2.83 (1.69-4.74)	<0.001	4.68 (2.45-8.89)	<0.001

Abbreviations: ALT, alanine aminotransferase; AST, aspartate transaminase; AFP, α-fetoprotein; BCLC, Barcelona Clinic Liver Cancer; HR, hazard ratio; N.A, not applicable.

Figures

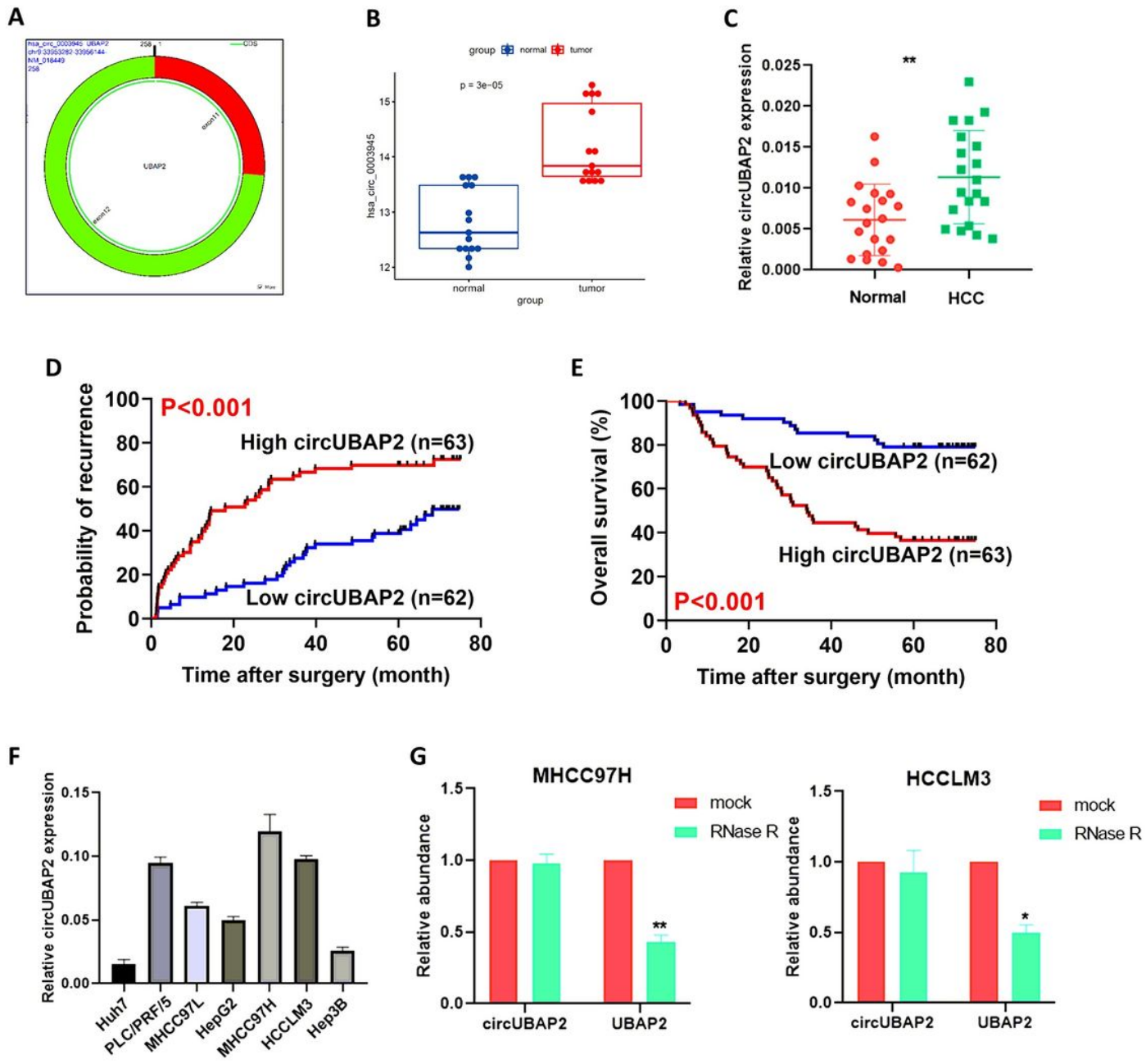

Figure 1

CircUBAP2 is highly upregulated in HCC tissues and is associated with poor outcomes. (A) Schematic illustration of the construction of circUBAP2. (B) CircUBAP2 expression levels in 15 HCC tissues and matched normal liver tissues based on bioinformatic analysis of a public database. (C) Validation of circUBAP2 expression in 20 HCC tissues and matched healthy liver tissues via qRT-PCR analysis. (D-E) Kaplan-Meier analyses were performed to analyze the correlation between circUBAP2 expression and OS as well as TTR in patients with HCC. (F) Detection of circUBAP2 expression levels in 7 HCC cell lines via qRT-PCR. (G) An RNase R treatment assay was conducted. Although circUBAP2 showed strong

exonuclease resistance, UBAP2 did not. Data are shown as the mean ± standard deviation of three independent experiments, and t-tests were used to compare group averages. **p < 0.01; ***p < 0.001.

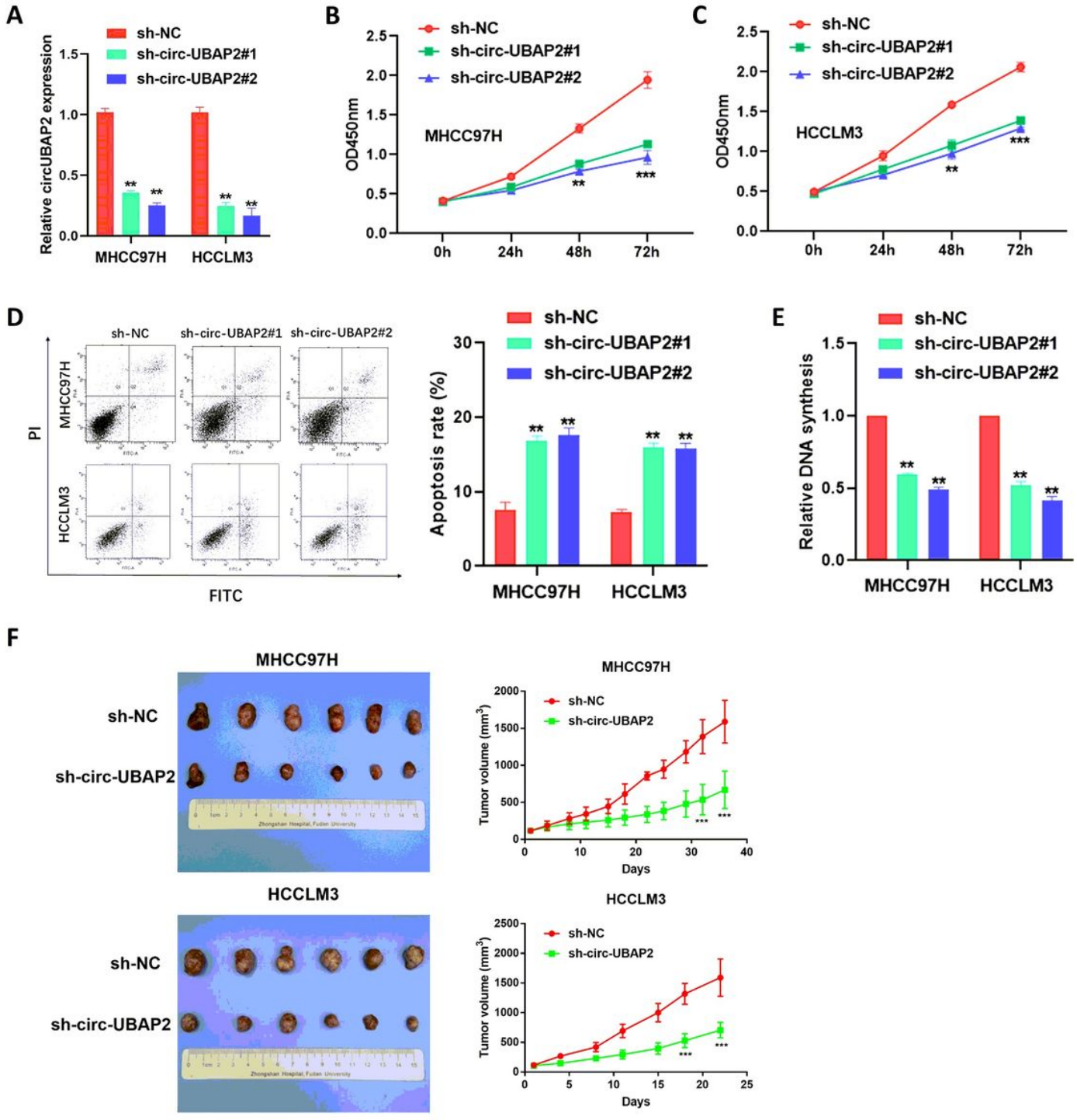

Figure 2

Knockdown of circUBAP2 inhibits liver cancer cell proliferation and induces cell apoptosis. (A) Confirmation of circUBAP2 knockdown (KD, sh-circ-UBAP2) in HCC cell lines by qRT-PCR. (B-C) CCK8 assays to detect the effects of circUBAP2 on HCC cell proliferation. (D-E) Flow cytometry showed that circUBAP2 inhibited HCC cell apoptosis and promoted DNA synthesis. (F) The effects of circUBAP2 gain-

or loss-of-function on in vivo HCC tumor size. Data are shown as the mean ± standard deviation of three independent experiments, and t-tests were used to compare group averages. **p < 0.01; ***p < 0.001.

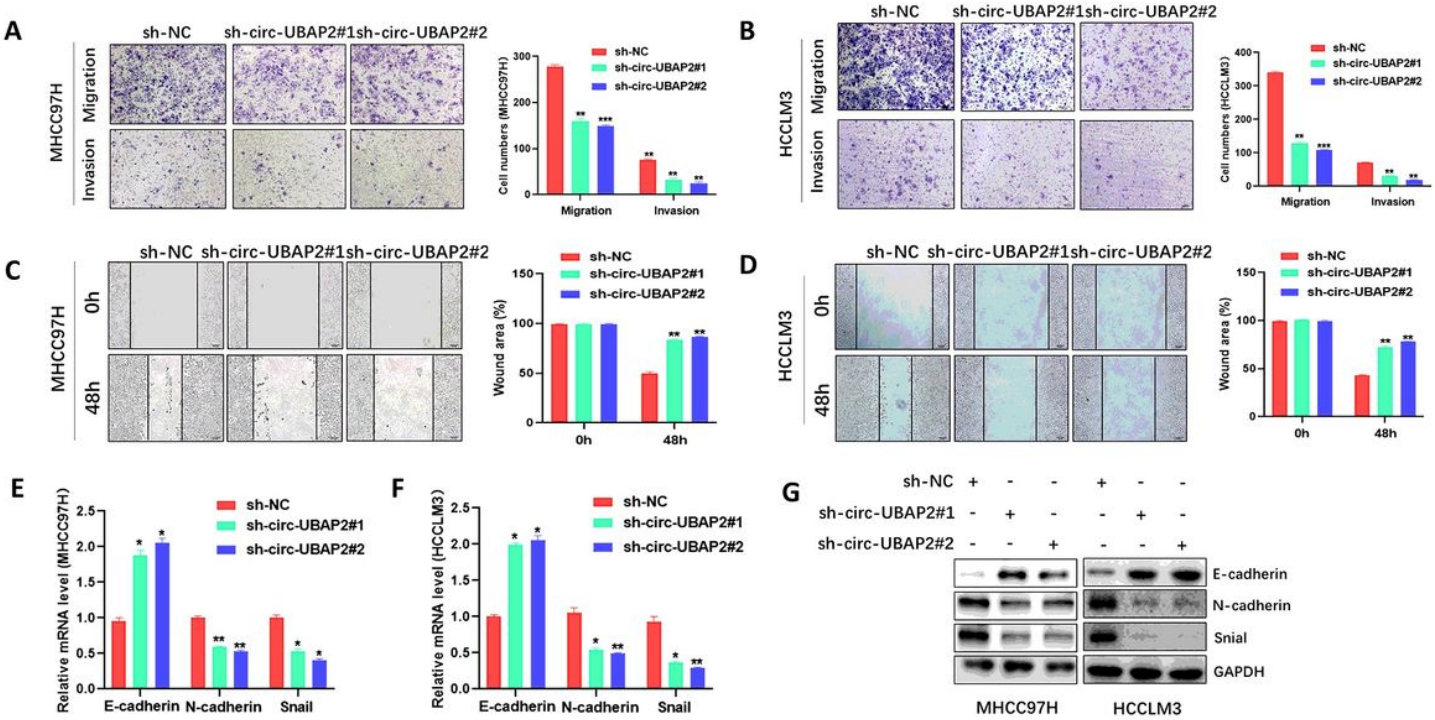

Figure 3

Knockdown of circUBAP2 suppressed migration and invasion in liver cancer cells. (A-B) Transwell migration and invasion assays were used to investigate the effects of circUBAP2 in HCCLM3 and MHCC97H cell lines. (C-D) Wound healing assays were used to evaluate the function of circUBAP2 in HCCLM3 and MHCC97H cell lines. (E) Expression of EMT-phenotype markers in HCCLM3 and MHCC97H cell lines after circUBAP2 downregulation were measured via qRT-PCR. (D) Expression of EMT-phenotype markers in HCCLM3 and MHCC97H cell lines after circUBAP2 downregulation were measured via WB. Data are shown as the mean ± standard deviation of three independent experiments, and t-tests were used to compare group averages. **p < 0.01; ***p < 0.001.

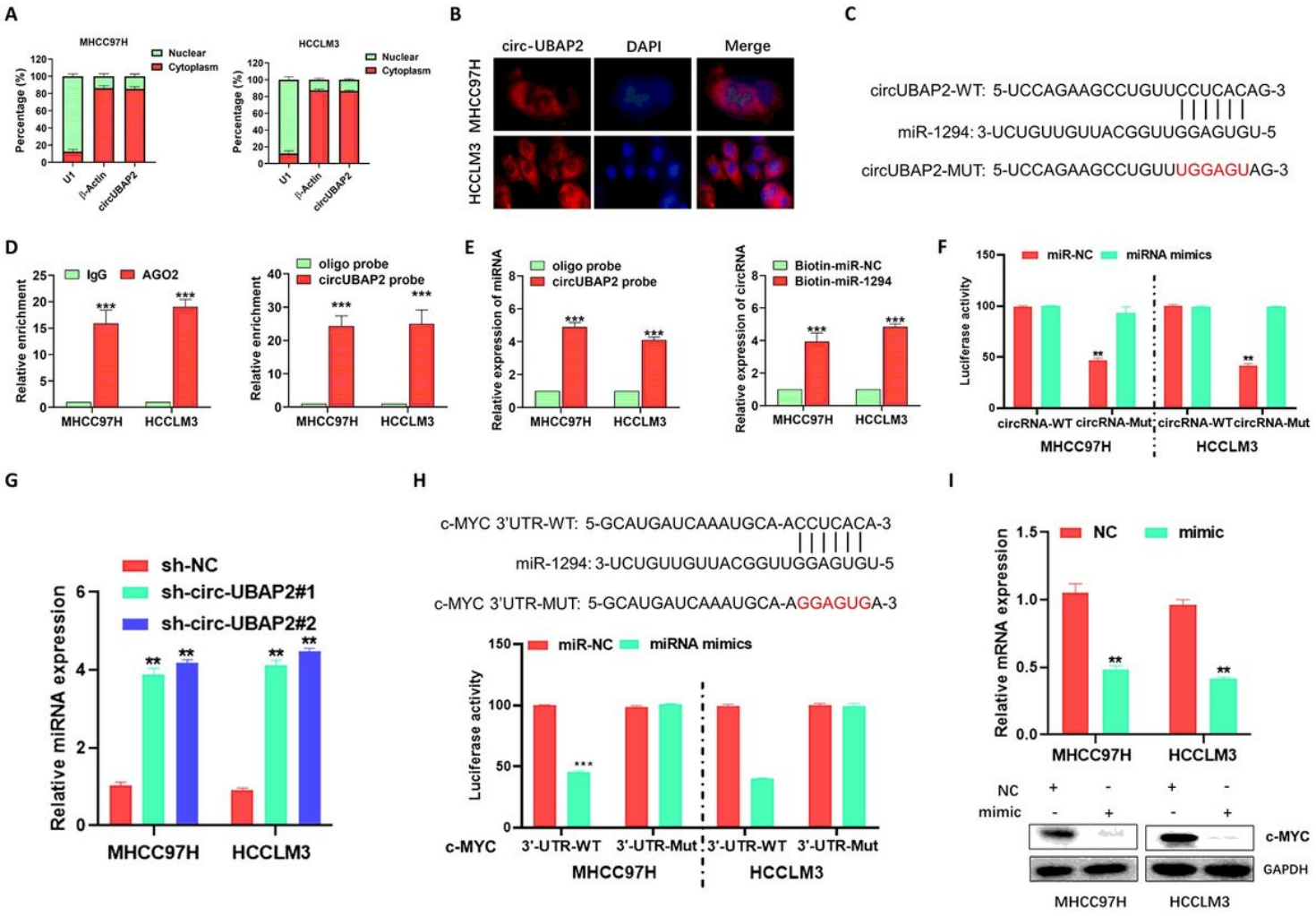

Figure 4

CircUBAP2 upregulated c-MYC expression by sponging miR-1294. (A-B) FISH and nuclear-plasma extraction assays were used to detect the localization of circUBAP2 in HCCLM3 and MHCC97H cell lines. (C) Bioinformatic analyses of the circRNA-miRNA-gene regulatory network. (D) RNA immunoprecipitation assays showed that circUBAP2 binds to AGO2 and confirmed the enrichment of circUBAP2 using a circUBAP2-specific probe. The enrichment of circUBAP2 was detected by qRT-PCR and normalized to that of a control probe. (E) RNA pull-down experiments were performed with HCCLM3 and MHCC97H cells using a circUBAP2-specific probe and biotin-labeled miR-1294 mimics. (F) qRT-PCR analysis showed that circUBAP2-KD cells had increased expression of miR-1294. (G) Dual-luciferase reporter assays were performed to measure the activity of LUC-circUBAP2 or LUC-circUBAP2-mutant in HCCLM3 and MHCC97H cell lines after overexpression of miR-1294. (H) Dual-luciferase reporter assays were performed to detect the activity of LUC-c-MYC or LUC-c-MYC-mutant in HCCLM3 and MHCC97H cell lines after overexpression of miR-1294. (I) qRT-PCR was combined with WB to show that treatment with an miR-1294 mimic decreased mRNA and protein levels of c-MYC. Data are shown as the mean ± standard deviation of three independent experiments, and t-tests were used. **p < 0.01; ***p < 0.001.

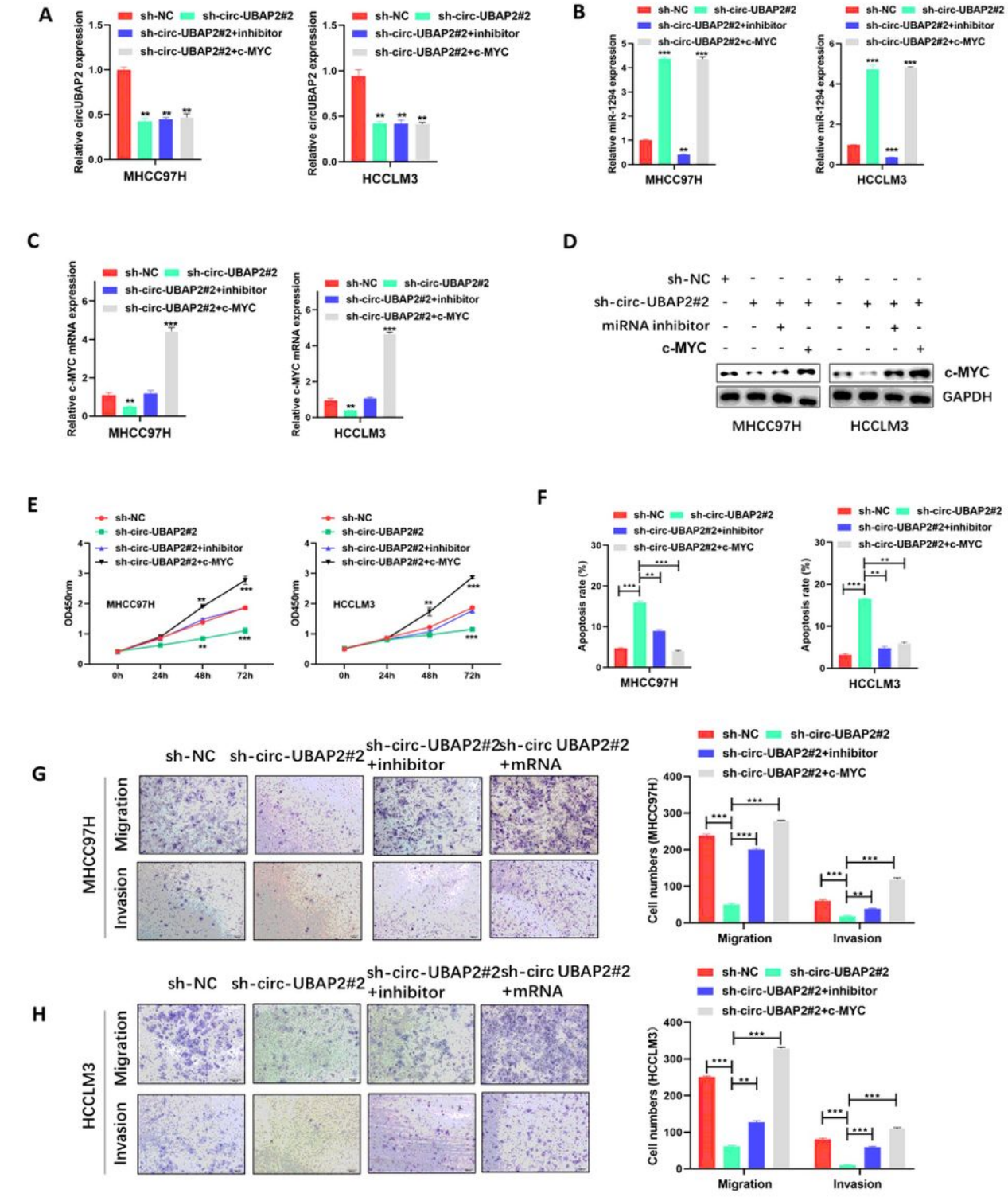

Figure 5

miR-1294 inhibitor and overexpression of c-MYC mRNA prevented the effects of circUBAP2 on liver cancer cells. (A-C) Relative expression of circUBAP2, miR1294, and c-MYC in MHCC97H and HCCLM3 cells after circUBAP2 knockdown, treatment with an miR-1294 inhibitor, and overexpression of c-MYC was quantified by qRT-PCR. (D) Relative expression of c-MYC in MHCC97H and HCCLM3 cells after circUBAP2 knockdown, treatment with an miR-1294 inhibitor, and overexpression of c-MYC was detected by WB. (E)

CCK8 assays found that an miR-1294 inhibitor reversed the effect of circUBAP2 knockdown on HCC proliferation. (F) Flow cytometry studies found that miR-1294 inhibitor attenuated the effects of circUBAP2 knockdown on HCC viability. Bar graphs represent the rate of apoptosis in treated cells. (G-H) MHCC97H and HCCLM3 cells were used to evaluate the effects of the miR-1294 inhibitor on HCC cell migration and invasion after circUBAP2 knockdown. Data are shown as the mean ± standard deviation of three independent experiments, and t-tests were used to compare group averages. **p < 0.01; ***p < 0.001.

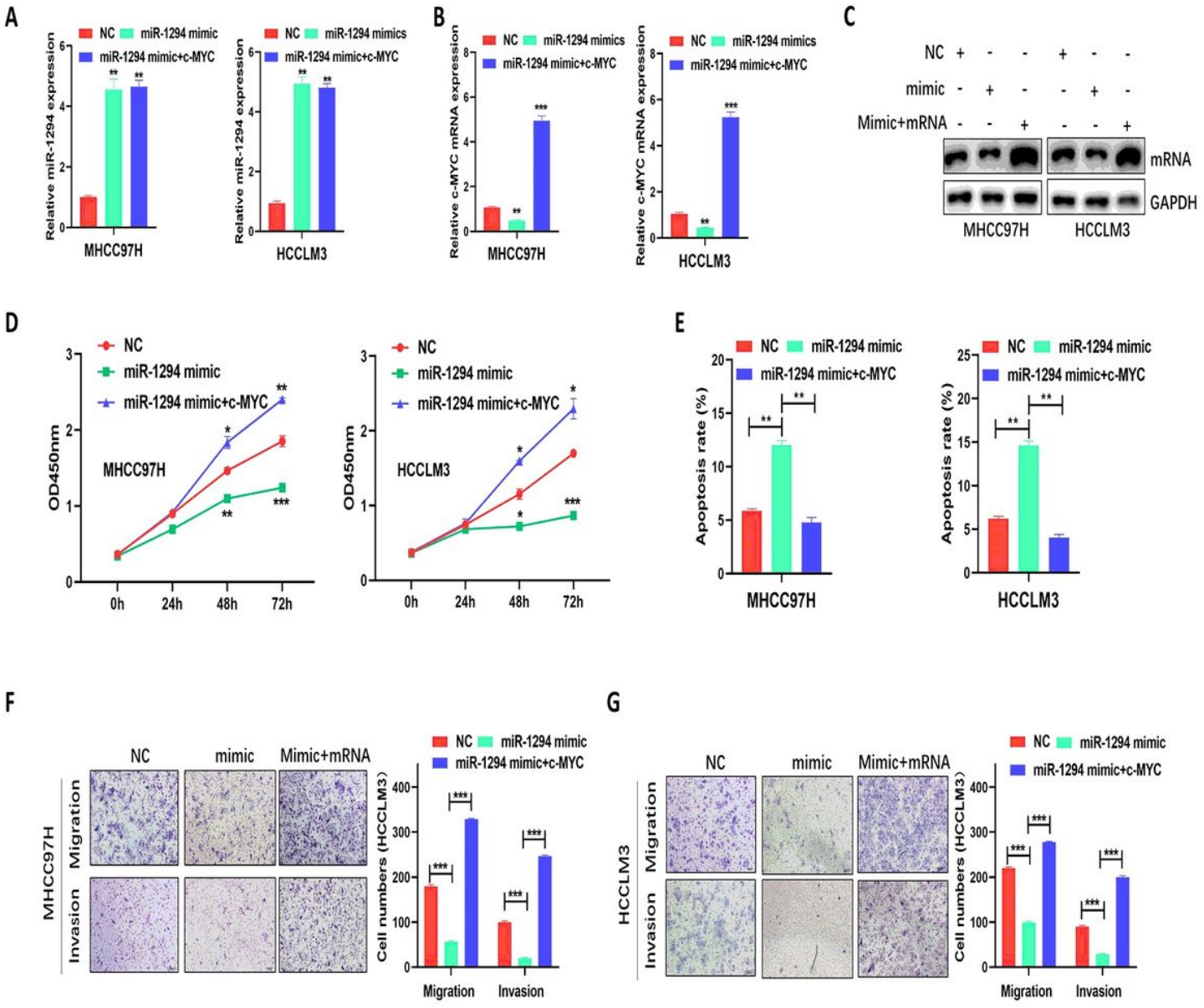

Figure 6

c-MYC overexpression rescues the tumor suppressive role of miR-1294 in HCC cells. (A) qRT-PCR showed that treatment with an miR-1294 mimic enhanced the relative expression of miR-1294. (B) qRT-PCR showed that miR-1294 overexpression decreased the expression of c-MYC mRNA. (C) Western blot

showed that miR-1294 overexpression decreased c-MYC protein expression. (D) c-MYC overexpression attenuated the effects of miR-1294 upregulation on HCC proliferation, as determined by CCK-8 assays. (E) c-MYC overexpression attenuated the effects of miR-1294 upregulation on HCC viability, as determined by flow cytometry assays. (F-G) c-MYC overexpression attenuated the effects of miR-1294 upregulation on HCC migration and invasion, as determined by transwell assays. Data are shown as the mean ± standard deviation of three independent experiments, and t-tests were used to compare group averages. **p < 0.01; ***p < 0.001.